1-1-2004

Magneto-Thermal Behavior of a Granular $FeCl_2$–Fe Heterostructure

Sarbeswar Sahoo
University of Nebraska-Lincoln, sarbeswar@gmail.com

Christian Binek
University of Nebraska-Lincoln, cbinek@unl.edu

Wolfgang Kleemann
Angewandte Physik, Universität Duisburg-Essen, 47048 Duisburg, Germany, wolfgang.kleemann@uni-due.de

Published in *Phase Transitions* 77:1–2 (January–February 2004), pp. 217–224. http://www.tandf.co.uk/journals/titles/01411594.asp

Magneto-Thermal Behavior of a Granular $FeCl_2$–Fe Heterostructure

S. Sahoo*, C. Binek and W. Kleemann

Angewandte Physik, Universität Duisburg-Essen, 47048 Duisburg, Germany

*Corresponding author: sahoo@kleemann.uni-duisburg.de

Abstract: A granular system consisting of ferromagnetic single-domain Fe particles in an antiferromagnetic $FeCl_2$ matrix was prepared by coevaporation in an ultra-high vacuum environment. The structural and magnetic properties were investigated by X-ray diffractometry and superconducting quantum interference device magnetometry, respectively. The heterostructure combines the properties of superparamagnetic Fe granules and the antiferromagnetism of the $FeCl_2$ matrix. In addition, dipolar interaction-induced giant moments are observed below the Néel temperature of the $FeCl_2$ matrix. The thermomagnetic properties of the giant moments are studied.

Keywords: Granular thin films; Dipolar interactions; Exchange coupling

1. INTRODUCTION

The macroscopic behavior of nanostructured magnetic systems is determined by the structure, size and morphology of the constituent materials and by the type and strength of magnetic coupling between them. For an assembly of noninteracting single-domain ferromagnetic (FM) particles, the magnetic properties mainly depend upon their volume. For instance, superparamagnetic single domain-particles embedded in an insulating matrix show blocking behavior when the thermal energy becomes comparable to the energy barrier which a supermoment has to overcome for reversal. The barrier is given by the anisotropy energy which is proportional to the particle volume (Dormann et al., 1997). Interparticle interactions (dipole–dipole or exchange type) compete with the anisotropy in determining the orientation of the particle moments. If strong enough, these interactions may turn the sum of individual superparamagnetic relaxation processes into a collective dynamic behavior (Dormann et al., 1998; Sahoo et al., 2002a). Furthermore, at sufficiently high packing densities, viz. at a magnetic volume fraction of about 40%, superferromagnetic features have been revealed (Sahoo et al., 2002b; Chen et al., 2000). It is important to mention that in such cases only interparticle interactions have been considered, while particle–matrix interactions have usually been neglected.

A less explored issue concerns the understanding of the magnetic behavior of systems where the nanoparticle–matrix interaction is effective. Most activities have originated from the pioneering work of Meiklejohn and Bean who, in 1956, discovered that Co nanoparticles embedded in their native oxide CoO possess a unidirectional anisotropy (Meiklejohn and Bean, 1956). This results in a shift of the hysteresis loop after field-cooling (FC) to below the Néel temperature of CoO. This phenomenon is known as exchange bias. Later on, the phenomenon was observed in many other FM-AF fine particle systems and in continuous films of sandwiched AF and FM thin layers (Nogués and Schuller, 1999). Recent experiments have confirmed that the spin alignment of the FM spins in these exchange-coupled systems is determined by the direction of the excess spins in the underlying AF layer giving rise to pinning of the ferromagnet and, hence, to exchange bias (Nolting et al., 2000).

On the other hand, retroactivity of the FM nanoparticles on the AF matrix may also be expected, if the AF intra-matrix exchange is weak compared to its interaction with the embedded FM nanoparticles. Related effects were recently observed (Binek et al., 2002) on an FePt/$FeCl_2$ heterostructure, where $FeCl_2$ is an Ising-type AF system whose interlayer AF coupling (J'/k_B = –0.18 K) is approximately twenty times weaker than the intra-layer FM exchange coupling between Fe^{2+} ions (J/k_B = 3:9K) (Jacobs and Lawrence, 1967). In this article we present the corresponding granular $FeCl_2$–Fe heterostructure which may be considered as a model system to study the retroactivity of Fe granules onto the $FeCl_2$ matrix. Apart from direct exchange coupling at the interface of the Fe granules and the Fe^{2+}-ions of $FeCl_2$ matrix, the dipolar stray-fields of the granules will play a key role in determining the magnetic properties of the system. It will be shown that under the combined effects of these two mechanisms, giant metamagnetic moments containing Fe granules as nucleation cores are observed. Moreover, the giant moment clusters can be shown to grow at the expense of the AF regions upon repeated field-cooling.

2. SAMPLE PREPARATION

Molecular beam epitaxy (MBE) allows the growth of high-purity thin films in an ultra-high vacuum (UHV) environment. The sample investigated in this study was prepared by coevaporation of $FeCl_2$ and Fe in a UHV (1×10^{-10} mbar) MBE chamber on a sapphire ($11\bar{2}0$) substrate. After rinsing in acetone the substrate was preheated to 600 K for 1 h in order to degas it and then cooled to and maintained at liquid N_2 temperature during the evaporation processes. As a result $FeCl_2$ becomes amorphous, which warrants tight embedding of the Fe particles during the growth. Upon room temperature annealing $FeCl_2$ eventually recrystallizes and recovers its original bulk properties (Kleemann and Hendel, 1983). The materials were evaporated from three different Knudsen cells, while their thicknesses were controlled by calibrated quartz oscillators. The growth rates of $FeCl_2$ and Fe were 0.1 and 0.04 nm/s, respectively. The pressure during deposition was better than 1×10^{-7} mbar. To ensure that Fe particles are completely embedded in a textured $FeCl_2$ matrix, first of all a 200 nm layer of $FeCl_2$ was deposited on the substrate followed by coevaporation of $FeCl_2$ and Fe up to a thickness of 500 nm. The sample was protected with a 50 nm-thick gold capping layer. In order to avoid the formation of FeAu

alloy-like nanoparticles, the gold layer was deposited after completely covering the Fe and $FeCl_2$ mixture with a continuous 200 nm-thick layer of $FeCl_2$.

3. STRUCTURAL PROPERTIES

Structural characterization of the film was carried out by ex situ X-ray diffraction (XRD) (Philips PW1730) using Cu-$K\alpha$ radiation ($\lambda = 0.15418$ nm). Figure 1 shows a comparison of the XRD patterns of $FeCl_2$–Fe film to that of the sapphire $(11\bar{2}0)$ substrate. Analysis of the XRD data by using the rhombohedral unit cell parameters of $FeCl_2$ reveals that (112) planes of $FeCl_2$ coincide with $(11\bar{2}0)$ planes of the substrate. Indeed, the presence of narrow and high (112) and (224) $FeCl_2$ lines at the Bragg angles $2\theta = 37.83°$ and 80.85° supports (112) textured growth. Simultaneously, (112) and (224) $FeCl_2$ lines originating from Cu-$K\beta$ radiation are also observed at $2\theta = 34°$ and 71.4° in the film diffractogram. Furthermore, some tendency (1%) towards (111) orientation of $FeCl_2$ is observed. The analysis suggests polycrystallinity of $FeCl_2$. Using Scherrer's formula, $D = 0.9\lambda/\beta\cos\theta$ (Cullity and Stock, 2001), where λ is the wavelength of Cu-$K\alpha$ radiation, β the full width at half maximum intensity of the peak, and θ the diffraction angle, the average crystalline size D was found to be $D_{FeCl_2}(112) \approx 80$ nm.

Analysis of the diffractogram gives only a minor indication of the presence of oriented Fe granules by a Bragg peak at $2\theta = 66°$ referring to (300) planes. A rough estimate from Scherrer's formula yields a diameter $D_{Fe}(300) \approx 10$ nm ($\beta = 2.5°$) immediately after the first warming up to room temperature ("virgin sample"). Their presence has been evidenced more convincingly from the magnetization data as will be shown later.

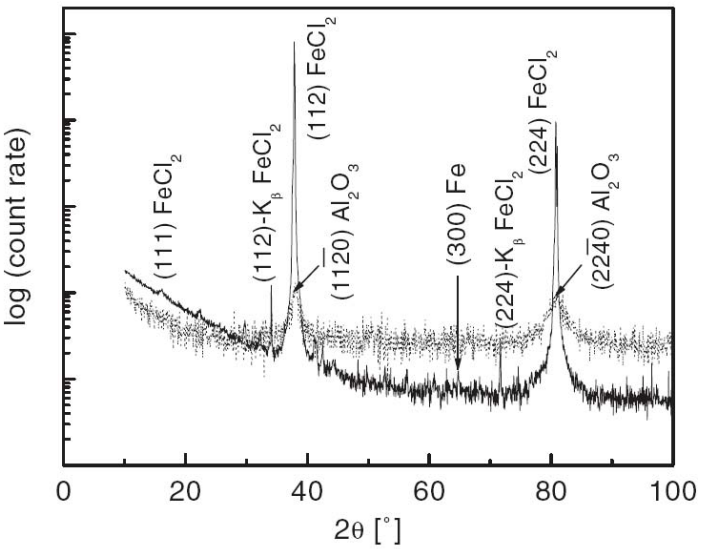

FIGURE 1 Comparison of the room temperature XRD pattern of an $FeCl_2$–Fe sample (solid line) to that of the sapphire substrate (dotted line) indicating some prominent Bragg peaks.

4. MAGNETIC PROPERTIES

DC-magnetization and ac-susceptibility measurements were performed by use of a commercial superconducting quantum interference device (SQUID) magnetometer (MPMS-5S, Quantum Design). For measurements of the zero field cooling-field heating (ZFC-FH) magnetization, $m^{\text{ZFC-FH}}$, the sample was cooled from high temperature (290 or 360 K) in zero field to 5 K, where a field step is applied and magnetization is recorded upon heating. Subsequent cooling in the same field gives rise to field-cooling (FC) magnetization, m^{FC}, while thermoremanent magnetization m^{TRM} is recorded during the following reheating after switching-off the field. In all measurements the sample was mounted with the external field oriented parallel to its plane.

Figure 2a shows the in-and out-of-phase components, χ' and χ'', respectively, of the ac-susceptibility measured on the virgin sample at a frequency $f = 20$ Hz and an ac amplitude $\mu_0 H_{\text{ac}} = 0.4$ mT. While no evidence of any AF features is present in χ'', a broad maximum of χ' around the anticipated Néel temperature gives a clear indication of the presence of $FeCl_2$ in the film. Similarly, a dc-magnetization measurement as shown in Fig. 2b involving an external magnetic field $\mu_0 H = 20$ mT confirms the presence of $FeCl_2$ with a sharp peak at $T_N = 22$ K and a rapid drop by $\approx 50\%$ with a minimum at $T \approx 12$ K. It should be noticed that T_N of our granular film is slightly below the bulk value of 23.7 K. Most remarkably, however, is a steep increase at low temperatures, $T < 10$ K. It reminds us of paramagnetic loose spins often encountered in disordered antiferromagnets, but probably refers to an extra magnetization due to the Fe nanoparticles. Their role becomes clearer when considering the heterostructure after aging at room temperature during more than three days.

In order to evidence the presence of the Fe particles in the "aged sample" we utilize the criterion of irreversibility between ZFC-FH and FC magnetizations, $m^{\text{ZFC-FH}}$ and m^{FC}, respectively, at the blocking temperature T_b. We identified it from the $m^{\text{ZFC-FH}}$ *vs* m^{FC} irreversibility occurring at $T \approx 320$ K as shown in the inset to Fig. 3(b). Clearly, this high value is incompatible with the XRD analysis on the virgin sample, since it corresponds to particles of diameter $D_{\text{Fe}} = 16$ nm as calculated from the Arrhenius-Néel-

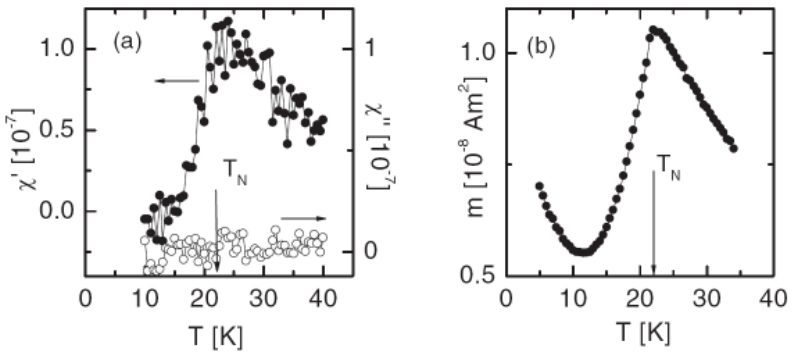

FIGURE 2 (a) ZFC ac-susceptibility *vs* temperature at an ac-amplitude $\mu_0 H = 0.4$ mT and frequency $f = 20$ Hz after few hours of exposure to room temperature. (b) ZFC magnetization *vs* temperature involving an external field $\mu_0 H = 20$ mT after few hours of exposure to room temperature. The arrows indicate the Néel temperature T_N .

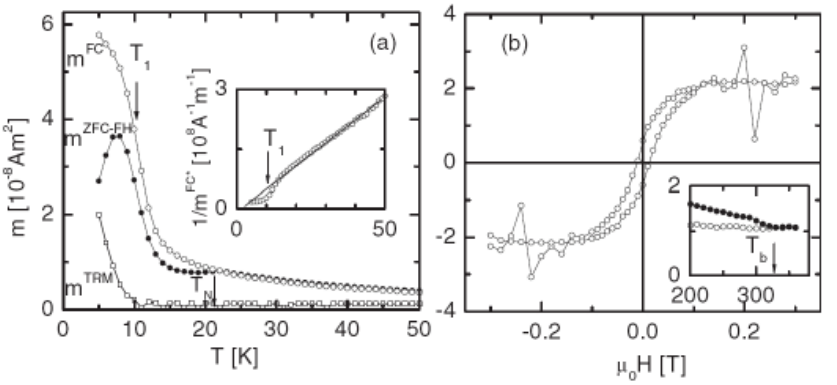

FIGURE 3 (a) $m^{\text{ZFC-FH}}$, m^{FC}, and m^{TRM} *vs* temperature, T, involving an external field $\mu_0 H =$ 10 mT after ZFC from $T =$ 290 K. The arrows indicate the corresponding Néel temperature, $T_N \approx 22$ K, and the point of inflexion, $T_1 \approx 10$ K, of m^{FC}. The inset shows $1/m^{\text{FC}}$ *vs* T and Curie-Weiss-type fit (straight line). (b) m *vs* $\mu_0 H$ loop at $T =$ 50 K. The inset shows the irreversibility between $m^{\text{ZFC-FH}}$ and m^{FC} (open and solid symbols, respectively) taking place at $T_b \approx 320$ K.

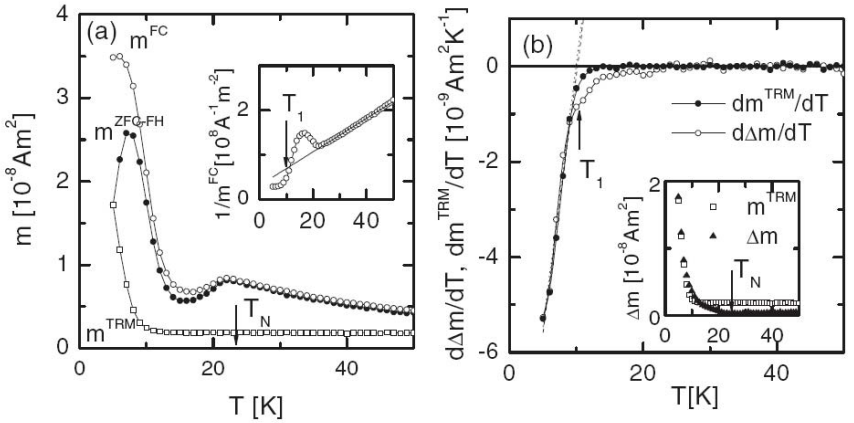

FIGURE 4 (a) $m^{\text{ZFC-FH}}$, m^{FC}, and m^{TRM} *vs* T involving an external field $\mu_0 H =$ 10 mT after a demagnetization procedure at $T =$ 290 K. (b) dm^{TRM}/dT and $d\Delta m/dT$ *vs* T, where $\Delta m = m^{\text{FC}} - m^{\text{ZFC}}$. The inset shows Δm and m^{TRM} *vs* T.

Brown blocking ansatz (Neel 1949; Brown 1963), $\tau = \tau_0 \exp(KV/k_B T)$, when associating an observation time of 100 s to our measurement. Here we have used $\tau_0 = 10^{-9}$ s and the value of the anisotropy constant $K = 5 \times 10^4$ Jm^{-3} for bulk Fe. Obviously, the result hints at coarse graining of the Fe granules in the early stage of our experiments which finally end up at $D_{\text{Fe}} =$ 16 nm. It is important to mention that all measurements carried out afterwards and described by Figs. 3–5 were reproducible.

Measurements of $m^{\text{ZFC-FH}}$, m^{FC}, and m^{TRM} involving an external field of $\mu_0 H = 10$ mT have been carried out under different starting conditions. The data shown in the main panel of Fig. 3(a) were obtained by starting in zero field at $T = 290 < T_b$. In this case, the

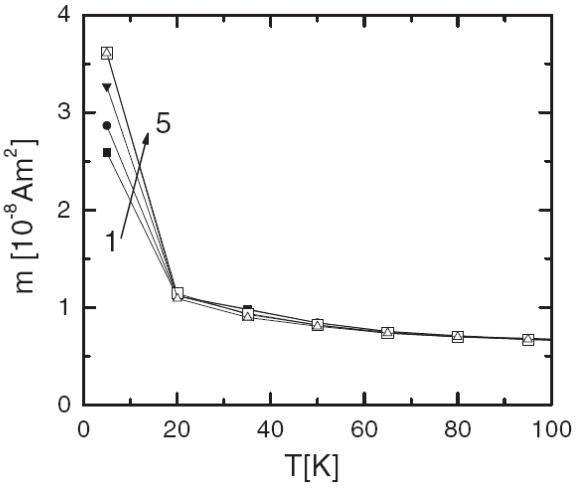

FIGURE 5 m^{FC} *vs* T in iterative cooling and heating cycles keeping the applied field constant at $\mu_0 H$ = 10 mT. The arrow indicates the sequence of cycles.

sample was in a premagnetized state, since the virgin sample was exposed to a magnetic field of 20 mT during a previous measurement shown in Fig. 2(b) after which these data were recorded without exceeding T_b. A similar set of measurements, but after a careful demagnetization procedure at T = 290 K, is shown in Fig. 4(a). In the demagnetization procedure, the sample is subjected to saturation in a field of 2 T which is then reduced to zero in an alternated cycle ("saturation-reverse-zero"). This procedure produces random orientations of the Fe moments and is considered to be equivalent to ZFC from above T_b.

Drastic changes in the properties of the aged sample are observed in both cases below $T < 15$ K. While the AF features, viz. a peak at the ordering temperature $T_N \approx 22$ K and a Curie-Weiss (CW)-type decrease at $T > T_N$ are retained, a pronounced peak at $T \approx 8$ K appears in $m^{ZFC\text{-}FH}$. This low temperature peak at $T \approx 8$ K arises due to the poor in-field alignment of randomly oriented blocked Fe moments which is partially lifted upon heating and gives rise to a decay at $T > 8$ K. Furthermore, a large enhancement in m^{FC} arises in the AF regime below $T \approx 15$ K. An accelerated increase of m^{FC} below the point of inflexion at $T_1 \approx 10$ K and saturation tendencies as $T \rightarrow 0$ seem to reflect metamagnetism of the $FeCl_2$ environment beyond the spin–flip transition (Jacobs and Lawrence 1967) which is induced by the field-aligned Fe granules.

It is remarked that m^{FC} in Fig. 3(a) shows no anomaly at the AF transition, which is more clearly seen when plotting $1/m^{FC}$ *vs* T (inset Fig. 3a). When fitted at $T > T_N$ to a CW-law, $m^{FC} = (C/(T - \theta_c))\mu_0 H$ (solid line), it yields $\theta_c = 2$ K. On the other hand, $1/m^{FC}$ *vs* T data shown in the inset of Fig. 4(a) when fitted similarly (solid line) yields $\theta_c = -9$ K. Obviously in the FC process of Fig. 3(a) starting from a premagnetized state, the blocked Fe granules convert a larger surrounding into an FM one by virtue of enhanced dipolar field strength.

Comparison of $m^{FC}(T = 5$ K) with the saturation moment of the magnetization hysteresis at $T = 50$ K $> T_N$ (Fig. 3b) shows that the total moment of the Fe granules is smaller ap-

proximately by a factor of three (Fig. 3a) or two (Fig. 4a) in order to explain its magnitude. These factors grow up to twelve (Fig. 3a) and seven (Fig. 4a), respectively, when comparing the remanence of the Fe granules (Fig. 3b) retained in the weak-field FC process with the low-T moments. Their origin, obviously, hints at an enhancement of the FM polarization by virtue of the AF matrix. Tentatively, we suggest the enhancement of the FM polarization within a model of "dressed" Fe granules (Sahoo et al., 2003). A polarization cloud is proposed to originate from FM exchange interaction between the spins of the field aligned Fe granules and the effective $S = 1$ spins of the Fe^{2+}-ions of the AF $FeCl_2$ matrix.

In Fig. 4(a), it is observed that m^{TRM} obeys the well-known rule of Stoner and Wohlfarth (1948) that the remanent magnetization, $m^{TRM}(T = 5K) = m_s/2$, where $m_s = m^{FC}(T = 5K)$ is the saturation value. Obviously also the "dressed" moments reorient onto the field-selected hemisphere in the same way as the bare SW particles are used to do (Stoner and Wohlfarth, 1948). Furthermore, m^{TRM} in both Figs. 3(a) and 4(a) decays rapidly to an almost constant value at $T > T_1$, referring to the remanence of the bare Fe nanoparticles. Obviously the lacking alignment of the Fe moments causes a destabilization of the metamagnetic coating at temperatures way below T_N. This is primarily due to the strong dependence of the spin–flip transition on the field orientation.

Further understanding on the stabilization of "dressed" moments can be extracted from two very useful quantities: $l = dm^{TRM}/dT$ and $m = d\Delta m/dT$, where $\Delta m = m^{ZFC\text{-}FH} - m^{FC}$. Both l and m exhibit almost similar trends with temperature as displayed in Fig. 4(b). When the temperature variation of Δm is compared to that of m^{TRM} (inset to Fig. 4b) it is found that they exhibit almost identical behavior at $T < T_1$. Linear extrapolations of the low temperature parts of l and m with the T-axis yield points of intersections close to T_1. Since m is a measure of the contribution of the polarized AF matrix and m^{TRM} achieves a constant value at $T < T_1$, these features indicate that the AF matrix stabilizes the "dressed" moments at $T < T_1$, where the dipolar field exceeds the spin–flip field of the AF matrix. Thermal disorder above T_1 randomizes the FM polarization and m^{TRM} attains the constant value of bare Fe granules.

Subsequent FC magnetization cycles further corroborate the above conjectured growth of the FM granules. To this end we measured m^{FC} in iterative cooling and heating cycles at constant $\mu_0 H = 10$ mT within $5 \leq T \leq 290$ K as shown in Fig. 5. It is seen that the FC-magnetization is reproducible down to $T = 20$ K, below which it shows an abrupt increase. In subsequent cycles the slope increases until the magnetization at 5 K approaches a constant value after the fourth cycle. Since the strength of the stray-field is proportional to the magnetic moment of the granule, the growth of granules is accompanied by increasing the stray-fields. On the other hand, a cut-off radius of the granules is finally determined by thermal disorder.

5. CONCLUSION

In summary, we have studied the structural and magnetic properties of Fe granules embedded in an $FeCl_2$ matrix and have shown that significant variations of their properties occur below the AF ordering temperature due to the presence of strong particle-matrix interac-

tion. We have demonstrated that giant moments of "dressed" Fe granules are formed below T_N and that they grow in repeated field-cooled cycles. The observations can be explained by assuming both exchange and dipolar coupling between the granules and the matrix.

Acknowledgements

This work was supported by the Deutsche Forschungsgemeinschaft within the framework of the Graduate School 277 "Structure and Dynamics of Heterogeneous Systems."

References

Binek, C., Hochstrat, A. and Kleemann, A. (2002). Domain state susceptibility in $FeCl_2$/CoPt heterostructures. *Phys. Stat. Sol.(a),* **189**, 575.

Brown, W.F. (1963). Thermal fluctuations of a single domain particle. *Phys. Rev.,* **130**, 1677.

Chen, X., Sichelschmidt, O., Kleemann, W., Petracic, O., et al. (2002). Domain wall relaxation, creep, sliding, and switching in superferromagnetic discontinuous $Co_{80}Fe_{20}$–Al_2O_3 multilayers. *Phys. Rev. Lett.,* **89**, 137203.

Cullity, B.D. and Stock, S.R. (2001). *Elements of X-Ray Diffraction.* Prentice Hall, New Jersey.

Dormann, J.L., Cherkaoui, R., Spinu, L., Nogués, M., et al. (1998). From pure superparamagnetic regime to glass collective state of magnetic moments in γ-Fe_2O_3 nanoparticle assemblies. *J. Magn. Magn. Mater.,* **187**, L139.

Dormann, J.L., Fiorani, D. and Tronc, E. (1997). Magnetic relaxation in fine particle systems. *Adv. Chem. Phys.,* **98**, 283.

Jacobs, I.S. and Lawrence, P.E. (1967). Magnetic phase transitions and hysteresis in $FeCl_2$. *Phys. Rev.,* **164**, 866.

Kleemann, W. and Hendel, B. (1983). X-ray and MCD investigations on amorphous thin films of $FeCl_2$. *J. Magn. Magn. Mater.,* **31–34**, 581.

Meiklejohn, W.H. and Bean, C.P. (1956). New magnetic anisotropy. *Phys. Rev.,* **105**, 904.

Néel, M.L. (1949). Théorie du trainage magnétique des ferromagnétiques engrains fins avec applications aux terres cuites. *Ann. de Geophys.,* **5**, 99.

Nogués, J. and Schuller, I.K. (1999). Exchange bias. *J. Magn. Magn. Mater.,* **192**, 203.

Nolting, F., Scholl, A., Stöhr, J., Seo, J.W., et al. (2000). Direct observation of the alignment of ferromagnetic spins by antiferromagnetic spins. *Nature,* **405**, 767.

Sahoo, S., Petracic, O., Binek, C., Kleemann, W., et al. (2002a). Superspin–glass nature of discontinuous $Co_{80}Fe_{20}/Al_2O_3$ multilayers. *Phys. Rev. B,* **65**, 134406.

Sahoo, S., Sichelschmidt, O., Petracic, O., Binek Ch., et al. (2002b). Magnetic states of discontinuous $Co_{80}Fe_{20}$-Al_2O_3 multilayers. *J. Magn. Magn. Mater.,* **240**, 433.

Sahoo, S., Binek, C. and Kleemann, W. (2003). Giant metamagnetic moments and exchange coupling in a granular $FeCl_2$–Fe heterostructure. *Phys. Rev. B.* (Submitted).

Stoner, E.C. and Wohlfarth, E.P. (1948). A mechanism of magnetic hysteresis in heterogeneous alloys. *Philos. Trans. London Ser. A,* **240**, 599.